

---

Title	Entanglement witness for spin glass
Author(s)	C. Y. Koh and L. C. Kwek
Source	<i>Physica A: Statistical Mechanics and its Applications</i> , 420, 324-330. <a href="http://dx.doi.org/10.1016/j.physa.2014.11.004">http://dx.doi.org/10.1016/j.physa.2014.11.004</a>
Published by	Elsevier

---

© 2015, Elsevier. Licensed under the Creative Commons Attribution-Non-Commercial-No Derivatives 4.0 International <http://creativecommons.org/licenses/by-nc-nd/4.0/>

This is the author's accepted manuscript (post-print) of a work that was accepted for publication in the following source:

Koh, C. Y., & Kwek, L. C. (2015). Entanglement witness for spin glass. *Physica A: Statistical Mechanics and its Applications*, 420, 324-330. <http://dx.doi.org/10.1016/j.physa.2014.11.004>

**Notice:** Changes introduced as a result of publishing processes such as copy-editing and formatting may not be reflected in this document. For a definitive version of this work, please refer to the published source.

# Entanglement Witness for Spin Glass

C. Y. Koh <sup>a</sup>, L. C. Kwek <sup>a,b</sup>

<sup>a</sup> Nanyang Technological University, National Institute of Education, 1, Nanyang  
Walk, Singapore 637616

<sup>b</sup> Department of Physics, National University of Singapore, 2 Science Drive 3,  
Singapore 117542

## Abstract

We derived the entanglement witness (EW) in Ising model for both the magnetic susceptibility and specific heat capacity of a spin glass. The magnetic susceptibility EW curve for  $\text{LiHo}_x\text{Y}_{1-x}\text{F}_4$  is formulated and compared with the existing data of  $\text{LiHo}_{0.167}\text{Y}_{0.833}\text{F}_4$  to identify the entangled and unentangled regions. The EW for the magnetic susceptibility was found to cut the cusp of the experimental result at a critical temperature of about 0.2669 K. The specific heat capacity EW curve for  $\text{Cu}_x\text{Mn}$  is formulated and compared with the existing data of  $\text{Cu}_{0.279}\text{Mn}$  to identify the entangled and unentangled region for the various applied magnetic field  $B$ . With increasing  $B$ , the critical temperature where the EW curve intersects the experimental data, increases as well.

# 1 Introduction

One of the long standing open question in the condensed matter physics is whether a spin glass has a new phase transition at certain critical temperature. Basically, a spin glass consists of anti-ferromagnetic and ferromagnetic spins which are randomly distributed in a non-magnetic material such as copper and gold. Due to the random positions of the spins, the alignment of the spins will tend to align in the configured energy of the ferromagnet or anti-ferromagnet depending on the neighboring spins. It is because of this nature of random positioning and usually at unequal distance apart that the frustration in the interaction occurs. These two features - disorder and frustration - form the very foundation of what is termed spin glass [1, 2, 3, 4, 5, 6, 7]. It is well known that liquid and gas contains atoms or molecules that move randomly and without any order in space. It is precisely because of this that statistical mechanics is able to describe the properties of liquid and gas theoretically with statistics and probability due to their symmetry nature. In contrast, spin glass do not contain atoms that move around in the alloy randomly. As a matter of fact, it is believed to be quenched or fixed in position over a time scale greater than the age of the universe. As a result, symmetry is broken and the knowledge of statistical mechanics is not able to fully describe the physics of a spin glass.

Experimental studies have shown that a typical spin glass exhibits a cusp in the magnetic susceptibility at certain critical temperature for low applied magnetic field. As most of these alloys contain a few percent of a magnetic element that is randomly

distributed in the non-magnetic host, the critical temperature at which this cusp appears varies according to the level of impurity concentration [8]. Examples of such diluted alloys are copper and manganese,  $\text{Cu}_{1-x} \text{Mn}_x$  [9] or gold and iron,  $\text{Au}_{1-x} \text{Fe}_x$  [10]. Other alloys with insulation and conduction properties which found to be spin glass are europium strontium sulfur  $\text{Eu}_x \text{Sr}_{1-x}\text{S}$  [11] and lanthanum gadolinium aluminum  $\text{La}_{1-x} \text{Gd}_x \text{Al}_2$  [12]. In general, all thermodynamic functions should in some way behave singularly when a phase transition has occurred [7, 13]. Therefore, the cusp in the magnetic susceptibility may suggest the occurrence of a phase transition. The effect of the sharp cusp becomes a broad maxima when a magnetic field of about 100 G is applied [10, 14, 15]. Besides being field dependent, some spin glasses are found to be frequency dependent [9, 16]. In contrast to the cusp in the susceptibility, the specific heat capacity of  $\text{Au}_{0.92} \text{Fe}_{0.08}$  [17] and  $\text{CuMn}$  [18] do not exhibit any sharp transition or singularity. Only a broad, smooth and rounded maximum is observed. In addition, the rounded maximum does not match the transition temperature of the magnetic susceptibility.

Based on the experimental results, models like the Edwards-Anderson (EA) [19] and Sherrington-Kirkpatrick (SK) [20] have been formulated in an attempt to understand the physics behind spin glass. The coupling in the EA model uses a random set of bonds that is usually taken from a Gaussian distribution. The random couplings represent site disorder and random Ruderman-Kittel-Kasuya-Yosida (RKKY) couplings [21, 22, 23]. Moreover, an asymmetric cusp is produced for both the magnetic susceptibility and specific heat capacity. Results by Fischer [24] have shown that the

theoretical specific heat does not always fit the experimental one. It is only true for low temperature linear dependence for spin  $S = \frac{1}{2}$ . In a bizarre manner, the SK model which manages to produce a cusp in the magnetic susceptibility and specific heat capacity, produced unphysical negative entropy. Due to the instability of the SK solution, Almeida and Thouless (AT) [25] divide the phase diagram for a spin glass into stable and unstable regions a line which is later named as the AT line. The instability of the solution was later found due to the treatment of all the replicas as indistinguishable. The unphysical negative entropy was later removed with the use of a replica symmetry breaking (RSB) scheme by Parisi [26, 27, 28, 29, 30]. Even then the method was found to be marginally stable. Despite the fact that different models and theories have been used to understand the physical nature of spin glass, there still remain many unaccounted experimental results which require a better theory to explain it. As all these theories have treated the spin glass in a classical sense, the quantization of the spins of the impurities are not taken into account [16]. However, the mathematical tools and new insights obtained in the study of spin glass were found to be useful in other areas of complex optimization problems [31], biological problems [32] and condensed matter [6, 5, 33]. In recent years, a quantum spin glass model of the form  $\text{LiHo}_x\text{Y}_{1-x}\text{F}_4$  has been extensively studied both experimentally and numerically [34, 35, 36, 37, 38, 39]. The magnetic  $\text{Ho}^{3+}$  ions in these materials behave like effective Ising spins while the yttrium  $\text{Y}^{3+}$  are non-magnetic ions. With an  $x$  concentration of  $\leq 0.25$ , a spin glass phase is found to exist. Nevertheless, it still remains as an open question of whether a spin glass or an anticlass spin phase

exists at lower concentration.

In the early development of quantum mechanics, the Einstein, Podolsky and Rosen [40] paradox has given rise to the notion of nonlocal realistic description of nature, bringing the idea of entanglement to the forefront. Recently, entanglement has been identified as a valuable resource for quantum information processing and it is used extensively in the study of phase transition for condensed matter physics. Moreover, the study of entanglement in both quantum information science and condensed matter physics forms an interesting connection between them [41, 42, 43, 44, 45, 46, 47]. Since entanglement describes the quantum correlations in a many body system, one raises the question of whether entanglement can be quantified at the macroscopic level [48, 49]. Indeed, many studies have been carried out in identifying the various experimental measurements used for the detection of entanglement in macroscopic system. This quantity is called entanglement witness (EW). Studies show that some thermodynamical properties like magnetic susceptibility, heat capacity and internal energy can be used as EW to detect entanglement between the individual particles of a solid [50, 51, 52]. The advantage of using such EW is that the measurements are applied at the macroscopic level. Some recent studies have used magnetic susceptibility and heat capacity as EW to quantify between the entangled and non-entangled regions by matching the experimental results of materials with the theoretical EW [50, 51, 53, 54, 55, 56, 57, 58]. Even though such studies have matched the EW successfully with the materials studied, little work has been carried out for spin glass. Moreover, the study of entanglement witness in spin glass is important due to

the following reasons: (i) to find out whether entanglement can be used as an order parameter to describe the quantum phase transition; (ii) to determine the limits of entanglement in terms of size for a spin glass; (iii) to find out if entanglement is a robust measurement in the presence of temperature. With this motivation, we attempt to use the EW for magnetic susceptibility and specific heat capacity in quantifying the entangled region from the non-entangled one for some known experimental results of the glassy materials.

The paper is organized as follows. We begin in subsection 2.1 by deriving the EW for magnetic susceptibility. The experimental results of the glassy materials are then plotted with the theoretical EW for the magnetic susceptibility. These results are presented and discussed in subsection 3.1. The same is carried out for the EW of the specific heat capacity in subsection 2.2 and the results discussed in subsection 3.2. In Sec. 4, we summarize our results and indicate some possible future directions.

## **2 Theoretical Formulation of Entanglement Witness**

### **2.1 Magnetic Susceptibility**

In this subsection, we follow the work of Wieśniak et al. [50] in deriving the magnetic susceptibility as a macroscopic entanglement witness. We briefly mentioned the derivation for the magnetic susceptibility here as the full work can be found in [50].

For an arbitrary state of spin  $S$  particle, one has

$$\langle (S_x)^2 \rangle + \langle (S_y)^2 \rangle + \langle (S_z)^2 \rangle = S(S+1) \quad (1)$$

and

$$\langle S_x \rangle^2 + \langle S_y \rangle^2 + \langle S_z \rangle^2 \leq S^2 \quad (2)$$

where  $S_x = \frac{\hbar}{2}\sigma_x$ ,  $S_y = \frac{\hbar}{2}\sigma_y$  and  $S_z = \frac{\hbar}{2}\sigma_z$ . In general, the Hamiltonian  $H = H_S + H_B$  can be used to describe any system as  $H_S$  is the spin Hamiltonian of a composite system consisting of  $N$  spins of an arbitrary spin length  $s$  in a lattice and  $H_B = B \sum_{i=1}^N S_a^i$ . The  $S_a^i$  ( $a = x, y, z$ ) refers to an  $a$ th component of the  $i$ th spin operator. The inclusion of the second term is to study its magnetic response properties, i.e. the solid is put in a weak magnetic field. However, the applied field  $B = 0$  is used in this study. Assuming that the density matrix  $\rho$  of the system is separable,

$$\rho = \sum W_n \rho_n^1 \otimes \rho_n^2 \otimes \cdots \otimes \rho_n^N \quad (3)$$

where  $N$  is the spin site,  $n$  denotes the different possible states and  $W_n$  is the probability of any classical mixture of the products states occurring. If each possible state is a separable state, therefore the entire system producing the different possible states is also separable. In statistical mechanics, the magnetic susceptibility is in general given as  $\chi = \beta (\langle M_z^2 \rangle - \langle M_z \rangle^2)$ , where  $\beta = \frac{1}{kT}$  and  $M$  is the magnetization. This can also be expressed as  $\frac{1}{kT} \left( \sum_{ij} \langle S_z^i S_z^j \rangle - \left\langle \sum_i S_z^i \right\rangle^2 \right)$  [13]. The magnetic susceptibility in



all 3 directions for the Heisenberg case is

$$\begin{aligned}
\chi_H &= \chi_x + \chi_y + \chi_z \\
&= \frac{1}{kT} \left[ \left( \sum \langle S_x^i S_x^j \rangle + \sum \langle S_y^i S_y^j \rangle + \sum \langle S_z^i S_z^j \rangle \right) \right. \\
&\quad \left. - \left( \langle \sum S_x^i \rangle^2 + \langle \sum S_y^i \rangle^2 + \langle \sum S_z^i \rangle^2 \right) \right] \tag{4}
\end{aligned}$$

For  $i = j$ ,  $\langle S_x^i \rangle^2 + \langle S_y^i \rangle^2 + \langle S_z^i \rangle^2 \leq \frac{\hbar^2}{4}$  and  $\langle (S_x^i)^2 \rangle + \langle (S_y^i)^2 \rangle + \langle (S_z^i)^2 \rangle = \frac{3\hbar^2}{4}$ .

Therefore, the magnetic susceptibility for spin  $S = \frac{1}{2}$  is

$$\begin{aligned}
\chi_H &= \chi_x + \chi_y + \chi_z \\
&= \frac{1}{kT} \left[ \left( \sum_{i=1}^N \frac{3\hbar^2}{4} - \sum_{i=1}^N \frac{\hbar^2}{4} \right) \right] \tag{5}
\end{aligned}$$

Since  $\langle S_x \rangle^2 + \langle S_y \rangle^2 + \langle S_z \rangle^2 \leq \frac{\hbar^2}{4}$ , therefore  $-\left(\langle S_x \rangle^2 + \langle S_y \rangle^2 + \langle S_z \rangle^2\right) \geq -\frac{\hbar^2}{4}$  and

$$\begin{aligned}
\chi_H &\geq \frac{1}{kT} \left[ \left( \sum_{i=1}^N \frac{3\hbar^2}{4} - \sum_{i=1}^N \frac{\hbar^2}{4} \right) \right] \\
&\geq \frac{1}{kT} \left( \frac{3N\hbar^2}{4} - \frac{N\hbar^2}{4} \right) \\
&\geq \frac{N\hbar^2}{2kT} \tag{6}
\end{aligned}$$

For the case of isotropic Heisenberg model,  $\chi_x = \chi_y = \chi_z$  and can simplify to  $3\chi_z$ .

Hence, the magnetic susceptibility for the Ising case is

$$\chi_I \geq \frac{N\hbar^2}{6kT} \tag{7}$$

In general, with spin  $S$  for the Ising model ,

$$\chi_I \geq \frac{NS\hbar^2}{3kT} \tag{8}$$

where  $N$  is the number of spins,  $T$  is the temperature,  $k$  is the Boltzmann constant and  $S$  is an arbitrary spin  $S$  particle.

## 2.2 Specific Heat Capacity

In this subsection, we follow the work of Wieśniak et al. [51] in deriving the heat capacity as a macroscopic entanglement witness. We briefly mentioned the derivation for the heat capacity and the full work can be referenced to [51]. The heat energy is given as

$$\begin{aligned}\Delta Q &= mc\Delta\theta \\ &= C\Delta\theta\end{aligned}\tag{9}$$

where  $Q$  is the heat energy,  $m$  is the mass of the sample,  $c$  is the specific heat capacity of the sample,  $\Delta\theta$  is the change in temperature. The heat capacity  $C$  of the sample is equivalent to mass  $m$  of the sample multiply by the specific heat capacity  $c$  of the sample. In thermodynamics,  $\Delta Q = \Delta U + P\Delta V$ . Since there is no change in volume ( $\Delta V = 0$ ),  $\Delta Q = \Delta U$ . The partition function is  $Z \equiv \text{tr}\left(e^{-\frac{H}{kT}}\right)$ , where  $H$  represents a general Hamiltonian,  $k$  is the Boltzmann constant and  $T$  is the temperature. The density matrix for the thermal state is  $\rho = \frac{e^{-\beta H}}{Z}$ . Since  $Z \equiv \text{tr}\left(e^{-\frac{H}{kT}}\right)$ ,

$$\frac{\partial \ln Z}{\partial \beta} = -\text{tr}\left(H \frac{e^{-\beta H}}{Z}\right)\tag{10}$$

Therefore,

$$-\frac{\partial \ln Z}{\partial \beta} = \langle H \rangle\tag{11}$$

Since the average Hamiltonian  $\langle H \rangle$  is equivalent to the internal energy  $U$ , therefore

$$\frac{\partial U}{\partial \beta} = -\frac{\partial^2 \ln Z}{\partial \beta^2} \quad (12)$$

In the limit  $\Delta\theta \rightarrow 0$ ,  $\frac{\Delta Q}{\Delta\theta} \approx C$  and  $C = \frac{\partial Q}{\partial T} = \frac{\partial U}{\partial T}$ . Hence, the heat capacity

$$C = \frac{1}{kT^2} \left( \frac{\partial^2 \ln Z}{\partial \beta^2} \right) \quad (13)$$

Since  $\frac{\partial \ln Z}{\partial \beta} = -\text{tr} \left( H \frac{e^{-\beta H}}{Z} \right)$ , then  $\frac{\partial}{\partial \beta} \left( \frac{\partial \ln Z}{\partial \beta} \right) \Rightarrow \frac{\partial^2 \ln Z}{\partial \beta^2}$  and

$$\begin{aligned} \frac{\partial}{\partial \beta} \left[ -\text{tr} \left( H \frac{e^{-\beta H}}{Z} \right) \right] &= -\text{tr} \left( \frac{\partial H}{\partial \beta} \frac{e^{-\beta H}}{Z} \right) - \text{tr} \left( H \frac{\partial (e^{-\beta H})}{\partial \beta} \frac{1}{Z} \right) \\ &\quad - \text{tr} \left[ H e^{-\beta H} \frac{\partial}{\partial \beta} \left( \frac{1}{Z} \right) \right] \end{aligned} \quad (14)$$

Since  $\frac{\partial H}{\partial \beta}$  is differentiating  $H$  which does not has  $\beta$  in it, therefore  $\frac{\partial H}{\partial \beta} = 0$  as differentiating a constant will be zero. Therefore,

$$\frac{\partial^2 \ln Z}{\partial \beta^2} = -\text{tr} \left[ H (-He^{-\beta H}) \frac{1}{Z} \right] - \text{tr} \left[ H e^{-\beta H} \frac{\partial}{\partial Z} \left( \frac{1}{Z} \right) \frac{\partial Z}{\partial \beta} \right] \quad (15)$$

For  $\text{tr} \left( H \frac{e^{-\beta H}}{Z} \right) = \text{tr}(\rho H)$ ,

$$\frac{\partial^2 \ln Z}{\partial \beta^2} = \langle H^2 \rangle - \langle H \rangle^2 \quad (16)$$

Therefore,  $\frac{\partial^2 \ln Z}{\partial \beta^2} = \Delta^2(H) \equiv \text{var}(H) \equiv (\Delta H)^2$ . Hence, the heat capacity

$$C = \frac{1}{kT^2} \Delta^2(H) \quad (17)$$

If  $H = H_{Ising}$  (where  $H_{Ising}$  is the Hamiltonian for Ising model), the eigenstate are not separable. The thermal state  $\rho = \frac{1}{Z} e^{-\beta H} = \frac{1}{Z} \sum e^{-\beta E_i} |E_i\rangle \langle E_i|$ , where  $|E_i\rangle \langle E_i|$

is entangled. Based on Wieśniak et al. [51], the variance is

$$\begin{aligned}\Delta^2(H_{Ising}) &= N(1 + z_1^2 + z_2^2 - 3z_1^2z_2^2) - 2BN[z_1z_2(x_1 + x_2)] \\ &\quad + B^2\frac{N}{2}(2 - x_1^2 - x_2^2)\end{aligned}\tag{18}$$

where  $x_i = \langle \psi_i | \sigma_x | \psi_i \rangle = \sin \theta_i$  and  $z_i = \langle \psi_i | \sigma_z | \psi_i \rangle = \cos \theta_i$ . In order to discuss the specific heat capacity in terms of per spin, Eq. (18) is expressed as

$$\begin{aligned}\frac{\Delta^2(H_{Ising})}{N} &= 1 + \cos^2 \theta_1 + \cos^2 \theta_2 - 3 \cos^2 \theta_1 \cos^2 \theta_2 \\ &\quad - 2B[\cos \theta_1 \cos \theta_2 (\sin \theta_1 + \sin \theta_2)] \\ &\quad + \frac{B^2}{2}(2 - \sin^2 \theta_1 - \sin^2 \theta_2)\end{aligned}\tag{19}$$

By numerical minimization with  $\theta_1$  and  $\theta_2$  over a random range of 0 to  $2\pi$ , the heat capacity per spin is

$$\frac{C}{N} = \frac{1}{kT^2} \frac{\Delta^2(H_{Ising})}{N}\tag{20}$$

## 3 Discussion and Results

### 3.1 Comparison of EW for Magnetic Susceptibility

As the magnetic susceptibility  $\chi_H$  is derived from a more general Hamiltonian of Heisenberg model as compared to the Ising model, we used the derived  $\chi_I$  in detecting the entanglement in the the dipolar-coupled Ising system  $\text{LiHo}_x\text{Y}_{1-x}\text{F}_4$  [59]. By varying the Ho (Holmium) to Y (Ytterbium) ratio, different levels of randomness can be introduced into the Ho spin system. According to Reich et al. [59], the compound

is ferromagnetic for Holmium concentrations of at least as low as  $x = 0.46$  and for  $x = 0.167$ , the sample behaves as a spin glass above its transition temperature. It supports a complex ground state with no appreciable gap, which is in accordance to the theories of spin glasses. Hence, we digitize the data points for the real part of the ac magnetic susceptibility  $\chi'$  as a function of temperature  $T$  at frequency  $f = 50$  Hz from the plot in the paper. Both the data points for cooling and warming of the  $\text{LiHo}_{0.167}\text{Y}_{0.833}\text{F}_4$  are plotted together with the derived magnetic susceptibility  $\chi$  to show the entangled and unentangled regions. In order to compare the theoretical magnetic susceptibility with the experimental results, the magnetic susceptibility is

$$\chi = \frac{10^6}{4\pi} \frac{M_m N g^2 \mu_B^2 S}{3kT} \quad (21)$$

where  $M_m$  is the molecular mass of the sample,  $N$  is the Avogadro's number,  $g$  is the Landé g-factor,  $\mu_B$  is the Bohr magneton and  $S$  is the spin number. All the universal constant are expressed in SI unit. According to Quilliam et al. [60], the magnetic Holmium  $\text{Ho}^{3+}$  ions in the  $\text{LiHo}_x\text{Y}_{1-x}\text{F}_4$  has spin  $S = 2$ ,  $g = \frac{5}{4}$ . The molecular mass of the sample is 184.545 g. The volume and mass of the sample is  $0.25 \text{ cm}^3$  and 1 g respectively. For  $\text{LiHo}_{0.167}\text{Y}_{0.833}\text{F}_4$ , the experimental results for the magnetic susceptibility  $\chi'$  of the sample by cooling and warming in zero applied magnetic field are plotted with the EW for susceptibility. This is shown in Fig. 1. The area under the EW curve represents the region where the states are entangled (E) and above as unentangled (UE).

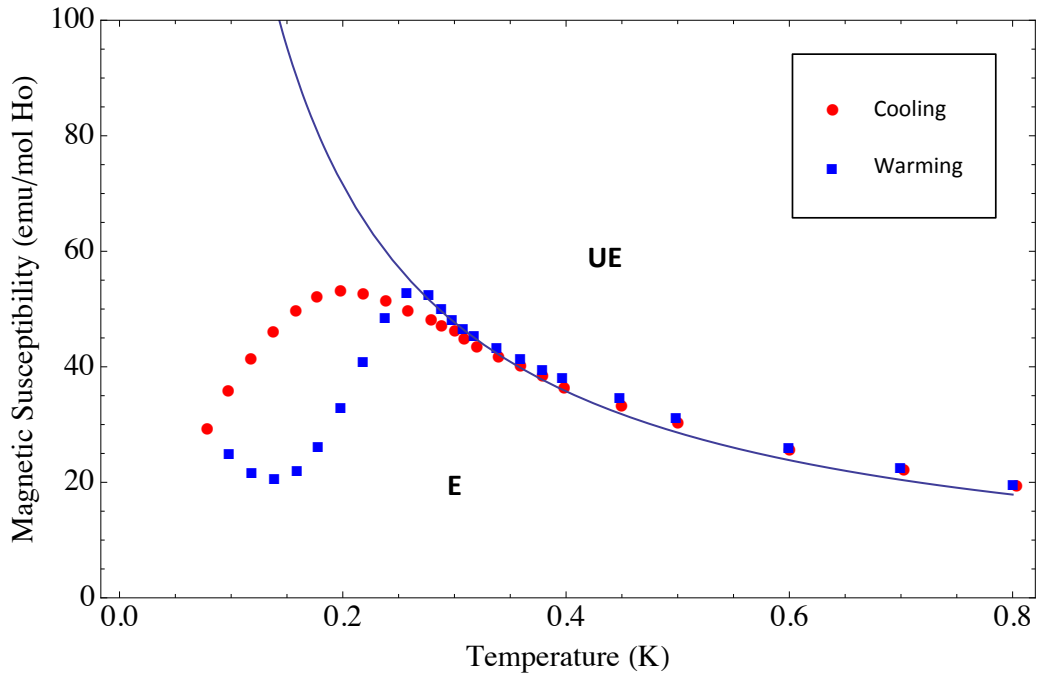


Figure 1: The curve represents the EW for magnetic susceptibility cutting through part of the experimental data points for the magnetic susceptibility of  $\text{LiHo}_{0.167}\text{Y}_{0.833}\text{F}_4$ .

### 3.2 Comparison of EW for Specific Heat Capacity

In this subsection, we compare the theoretical EW for specific heat capacity with the experimental results of  $\text{Cu}_x\text{Mn}$  [61]. The measurements for the heat capacity of  $\text{Cu}_x$  have shown the specific heat anomaly associated with the transition to the spin glass phase. The freezing temperature  $T_f$  is found to be at 3.89 K. The EW for the specific heat capacity will be used to compare with the results for  $\text{Cu}_x\text{Mn}$  with an applied magnetic field of range from approximately 1 T to 7.5 T. We modeled the sample

using the Ising model in a transverse magnetic field [62] which is given by

$$H_{Ising} = \sum_{i=1}^N J\sigma_i^z\sigma_{i+1}^z + B \sum_{i=1}^N \sigma_i^x \quad (22)$$

where  $J$  is the random coupling between  $i$  sites and  $B$  is the applied magnetic field. In order to compare the theoretical EW for specific heat capacity with the experimental results, Eq. (20) is reexpressed as

$$c = \frac{\Delta^2(H_{Ising})}{10^3 c_x N k T^2} \quad (23)$$

where  $c_x$  is the % concentration of Copper (Cu) in the sample and  $N$  is the Avogadro's number. The % concentration of the sample is 0.279. All the universal constants are expressed in SI unit. As  $\Delta^2(H_{Ising})$  is dependent on the applied magnetic field  $B$ , the minimization is carried out for  $B = (7.5, 6, 4.5, 3, 2, 1)$ T in order to obtain the minimized  $\Delta^2$ . For  $B = (7.5, 6, 4.5)$ T, the minimized  $\Delta^2 \approx 1T$ . For  $B = (3, 2, 1)$ T, the minimized  $\Delta^2 \approx (0.9230, 0.4197, 0.04891)$ T respectively. The different  $\Delta^2$  values corresponding to the different  $B$  are used to determine the EW for specific heat capacity.

For  $B \approx 1T$ , the EW is plotted together with the experimental results of  $\text{Cu}_{0.279}\text{Mn}$  as shown in Fig. 2(a). The states below the curve are entangled (E) and those above are unentangled (UE). Hence, values below the red dashed curve requires entanglement to explain and those above do not need. Similarly, for  $B \approx 2T$  and  $3T$ , the EW curve cuts through the experimental results differentiating the states which are entangled and unentangled as shown in Fig. 2(b) and Fig. 2(c) respectively. For  $B \approx (4.5, 6, 7.5)$ T, the EW curve for all the different applied magnetic field is the

same as represented in Fig. 2(d). As the magnetic field increases, the experimental results for  $\text{Cu}_{0.279}\text{Mn}$  at  $B \approx (4.5, 6, 7.5)$  seems to align closer together as compared to lower  $B$ . As observed from Fig. 2(a) to (d), the EW shifted away from the origin as the magnetic field increases. This is in agreement with Wieśniak et al. [51] that with increasing strength of  $B$ , the critical temperature below which entanglement is detected increases as well.

## 4 Conclusion

In this paper, we derived the EW for both magnetic susceptibility and specific heat capacity of a spin glass. We compare the experimental results for the  $\text{LiHo}_{0.167}\text{Y}_{0.833}\text{F}_4$  and  $\text{Cu}_{0.279}\text{Mn}$  with the derived magnetic susceptibility and specific heat capacity respectively. The EW for magnetic susceptibility was found to cut the cusp of the experimental data points for warming, giving the critical temperature at about 0.2669 K. This sort of critical temperature is also found in a study by Brukner et al. [54]. Below the EW curve marks the region where entanglement exists and above as unentangled region. The EW for the specific heat capacity varies with different applied magnetic field  $B$  and is dependent on  $B$ . Similar to the magnetic susceptibility for spin glass, the EW also cuts the experimental results for the  $\text{Cu}_{0.279}$  with different  $B$ . The intersection of the EW curve and the experimental data points for specific heat capacity divides the entangled region (below the EW curve) from the unentangled region (above the EW curve). It is found that with increasing  $B$ , the critical tem-



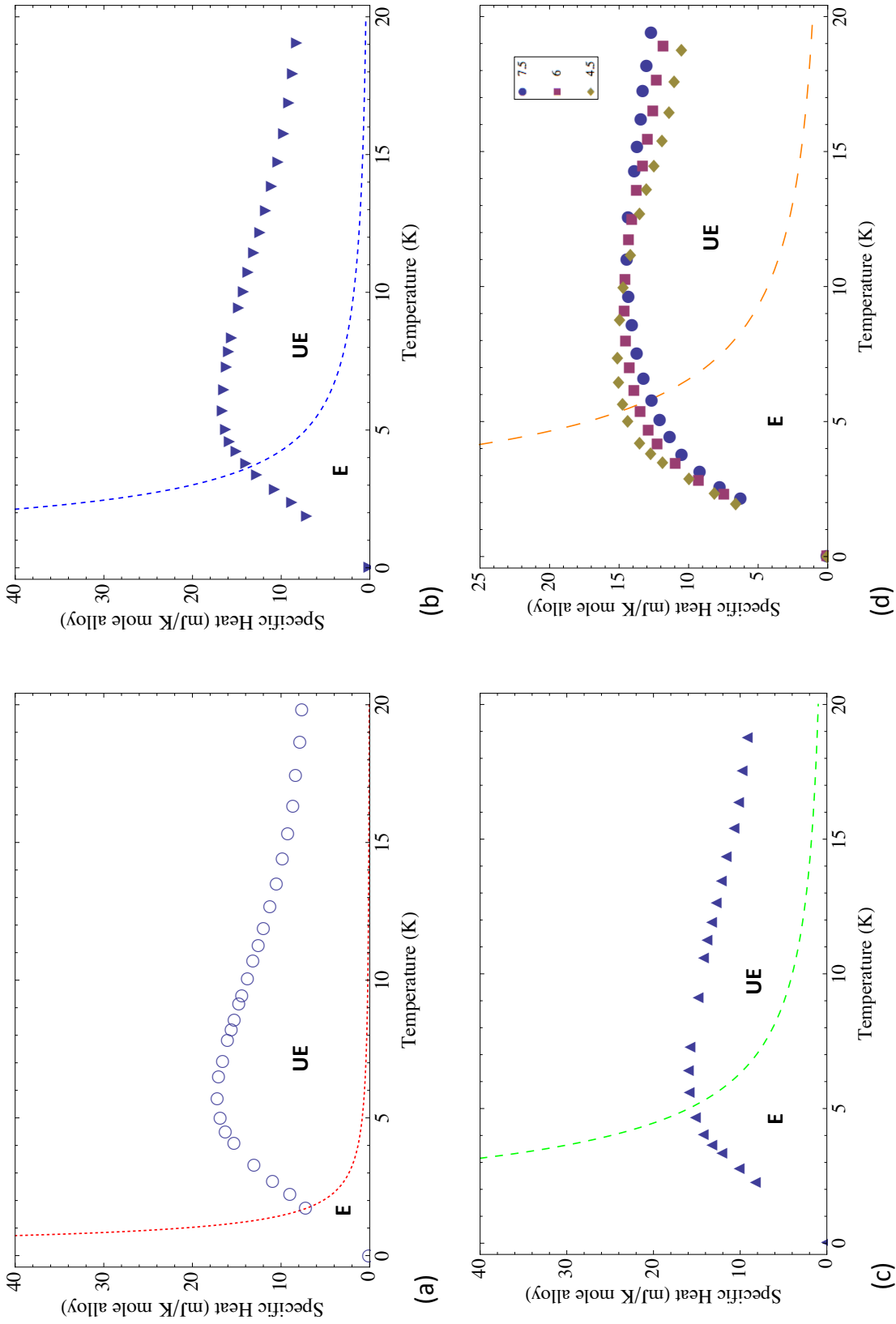


Figure 2: (a), (b), (c) and (d) show 4 different dashed lines representing the EW for heat capacity with different applied magnetic field of 1T, 2T, 3T and (4.5, 6, 7.5)T respectively. Corresponding to the various applied magnetic field, the experimental data points in (a), (b), (c) and (d) represents the specific heat capacity for  $\text{Cu}_{0.279}\text{Mn}$ .

perature (where the EW curve intersects the experimental data points) increases as well. Even though much studies have been carried out for non-spin glass materials, little work has been done on defining the EW for spin glass and comparing the derived EW with the experimental data of a spin glass. Since theories for spin glass are not able to fully explain the experimental results, this work shows that the theory of entanglement maybe needed to fully describe the cusp in the magnetic susceptibility and the heat capacity anomaly associated with a spin glass. As many classical experimental results of spin glass lack of information on the spin type, mass and density, future work may require more experimental results on spin glass with such measured quantities in order to compare with the theoretical aspects of entanglement witness. Moreover, the experiment should be carried out at temperature near to zero Kelvin since entanglement is best observed at low temperature.

## 5 Acknowledgement

This work is supported by the National Research Foundation and Ministry of Education, Singapore.

## References

- [1] K. Binder and A. P. Young, *Rev. Mod. Phys.* **58**, 801 (1986).
- [2] J. A. Mydosh and G. J. Nieuwenhuys (Elsevier, 1980) p. 71.

- [3] J. A. Mydosh, *J. Magn. Magn. Mater.* **7**, 237 (1978).
- [4] K. H. Fischer, *Phys. Status Solidi B* **116**, 357 (1983).
- [5] K. H. Fischer, H. Konrad, and J. A. Hertz, *Spin glasses*, Vol. 1 (Cambridge University Press, 1993).
- [6] J. A. Mydosh and T. W. Barrett, *Spin glasses: An experimental introduction*, Vol. 125 (Taylor & Francis London, 1993).
- [7] D. L. Stein and C. M. Newman, *Spin glasses and complexity* (Princeton University Press, 2013).
- [8] C. Y. Huang, *J. Magn. Magn. Mater.* **51**, 1 (1985).
- [9] C. A. M. Mulder, A. J. V. Duynveldt, and J. A. Mydosh, *Phys. Rev. B* **23**, 1384 (1981).
- [10] V. Cannella and J. A. Mydosh, *Phys. Rev. B* **6**, 4220 (1972).
- [11] H. Maletta and W. Felsch, *Phys. Rev. B* **20**, 1245 (1979).
- [12] J. Aarts, W. Felsch, H. V. Löhneysen, and F. Steglich, *Zeitschrift für Physik B Condensed Matter* **40**, 127 (1980).
- [13] F. Schwabl, *Statistical Mechanics* (Springer, 2003).
- [14] J. L. Tholence and R. Tournier, *Le Journal de Physique Colloques* **35**, C4 (1974).
- [15] O. S. Lutes and J. L. Schmidt, *Phys. Rev.* **134**, A676 (1964).

- [16] P. J. Ford, *Contemp. Phys.* **23**, 141 (1982).
- [17] L. E. Wenger and P. H. Keesom, *Phys. Rev. B* **11**, 3497 (1975).
- [18] L. E. Wenger and P. H. Keesom, *Phys. Rev. B* **13**, 4053 (1976).
- [19] S. F. Edward and P. W. Anderson, *J. Phys. F* **5**, 965 (1975).
- [20] D. Sherrington and S. Kirkpatrick, *Phys. Rev. Lett.* **35**, 1792 (1975).
- [21] T. Kasuya, *Prog. Theor. Phys.* **16**, 45 (1956).
- [22] K. Yosida, *Phys. Rev.* **106**, 893 (1957).
- [23] M. A. Ruderman and C. Kittel, *Phys. Rev.* **96**, 99 (1954).
- [24] K. H. Fischer, *Phys. Rev. Lett.* **34**, 1438 (1975).
- [25] J. R. L. de Almeida and D. J. Thouless, *J. Phys. A* **11**, 983 (1978).
- [26] G. Parisi, *J. Phys. A* **13**, L115 (1980).
- [27] G. Parisi, *Phys. Rev. Lett.* **43**, 1754 (1979).
- [28] G. Parisi, *J. Phys. A* **13**, 1887 (1980).
- [29] G. Parisi, *Philos. Mag. B* **41**, 677 (1980).
- [30] G. Parisi, *J. Phys. A* **13**, 1101 (1980).
- [31] S. Kirkpatrick, C. D. Gelatt, and M. P. Vecchi, *Science* **220**, 671 (1983).

- [32] J. J. Hopfield and D. W. Tank, *Biol. Cybern* **52**, 141 (1985).
- [33] H. Nishimori, *Statistical physics of spin glasses and information processing: An introduction*, 111 (Clarendon Press, 2001).
- [34] C. Ancona-Torres, D. M. Silevitch, G. Aeppli, and T. F. Rosenbaum, *Phys. Rev. Lett.* **101**, 057201 (2008).
- [35] J. A. Quilliam, S. Meng, C. G. A. Mugford, and J. B. Kycia, *Phys. Rev. Lett.* **101**, 187204 (2008).
- [36] A. Biltmo and P. Henelius, *Phys. Rev. B* **76**, 054423 (2007).
- [37] H. M. Rønnow, R. Parthasarathy, J. Jensen, G. Aeppli, T. F. Rosenbaum, and D. F. McMorrow, *Science* **308**, 389 (2005).
- [38] A. Biltmo and P. Henelius, *Phys. Rev. B* **78**, 054437 (2008).
- [39] K.-M. Tam and M. J. P. Gingras, *Phys. Rev. Lett.* **103**, 087202 (2009).
- [40] A. Einstein, B. Podolsky, and N. Rosen, *Phys. Rev.* **47**, 777 (1935).
- [41] L. Amico, R. Fazio, A. Osterloh, and V. Vedral, *Rev. Mod. Phys.* **80**, 517 (2008).
- [42] R. Horodecki, P. Horodecki, M. Horodecki, and K. Horodecki, *Rev. Mod. Phys.* **81**, 865 (2009).
- [43] C. Y. Koh, L. C. Kwek, S. T. Wang, and Y. Q. Chong, *Laser Physics* **23**, 025202 (2013).

- [44] C. Y. Koh, *Int. J. Mod Phys B* **28**, 1430012 (2014).
- [45] C. Y. Koh and L. C. Kwek, *Physica A* **403**, 54 (2014).
- [46] C. Y. Koh and L. C. Kwek, Submitted to *J. Magn. Magn. Mater.* .
- [47] C. Y. Koh and L. C. Kwek, *Phys. Lett. A* **378**, 2743 (2014).
- [48] V. Vedral, *Nature* **453**, 1004 (2008).
- [49] L.-A. Wu, S. Bandyopadhyay, M. S. Sarandy, and D. A. Lidar, *Phys. Rev. A* **72**, 032309 (2005).
- [50] M. Wieśniak, V. Vedral, and C. Brukner, *New J. Phys.* **7**, 258 (2005).
- [51] M. Wieśniak, V. Vedral, and C. Brukner, *Phys. Rev. B* **78**, 064108 (2008).
- [52] M. R. Dowling, A. C. Doherty, and S. D. Bartlett, *Phys. Rev. A* **70**, 062113 (2004).
- [53] G. Tóth, *Phys. Rev. A* **71**, 010301 (2005).
- [54] Č. Brukner, V. Vedral, and A. Zeilinger, *Phys. Rev. A* **73**, 012110 (2006).
- [55] C. De, Č. Brukner, R. Fazio, G. M. Palma, and V. Vedral, *New J. Phys.* **8**, 95 (2006).
- [56] A. M. Souza, M. S. Reis, D. O. Soares-Pinto, I. S. Oliveira, and R. S. Sarthour, *Phys. Rev. B* **77**, 104402 (2008).

- [57] T. Chakraborty, H. Singh, D. Das, T. K. Sen, and C. Mitra, *Phys. Lett. A* **376**, 2967 (2012).
- [58] H. Singh, T. Chakraborty, D. Das, H. S. Jeevan, Y. Tokiwa, P. Gegenwart, and C. Mitra, *New J. Phys.* **15**, 113001 (2013).
- [59] D. H. Reich, B. Ellman, J. Yang, T. F. Rosenbaum, G. Aeppli, and D. P. Belanger, *Phys. Rev. B* **42**, 4631 (1990).
- [60] J. A. Quilliam, S. Meng, and J. B. Kycia, *Phys. Rev. B* **85**, 184415 (2012).
- [61] G. E. Brodale, R. A. Fisher, W. E. Fogle, N. E. Phillips, and J. V. Curen, *J. Magn. Magn. Mater.* **31**, 1331 (1983).
- [62] B. Boechat, S. Dos, R. Raimundo, and M. A. Continentino, *Phys. Rev. B* **49**, 6404 (1994).